



Extending the wavelength tunability from 2.01 to 2.1 μm and simultaneous dual-wavelength operation at 2.05 and 2.3 μm in diode-pumped Tm:YLF lasers

Yunshan Zhang^a, Yaqi Cai^a, Bin Xu^{a,*}, Yilun Yang^b, Yin Hang^{b,**}

^a Department of Electronic Engineering, Xiamen University, Xiamen, 361005, China

^b Key Laboratory of Materials for High Power Laser, Shanghai Institute of Optics and Fine Mechanics, Chinese Academy of Sciences, Shanghai, 201800, China

ARTICLE INFO

Keywords:

Tm:YLF laser

Tunable laser

Passive Q-switching

ABSTRACT

We report on wavelength extension of diode-pumped Tm:YLF crystal lasers. Using specifically coated end-face mirrors, we have achieved a simultaneous dual-wavelength laser at 2.05 and 2.3 μm with a maximum output power up to 1.33 W and slope efficiency of about 9.7% in continuous-wave regime, for the first time to the best of our knowledge. Moreover, using an un-doped YAG etalon for wavelength tuning, the 2.05 μm lasing wavelength can be shifted to as far as 2.1 μm . We believe that it is the first time that a Tm:YLF laser has been wavelength extended to that far. Using a Cr:ZnSe saturable absorber, a passively Q-switched Tm:YLF laser at 2.05 μm has also attained with a maximum average output power of 0.66 W. The shortest pulse width is 91.7 ns at pulse repetition rate of 8.47 kHz. This work has extended the operating wavelengths of Tm³⁺ lasers to that in general for Ho³⁺ lasers, which could be practically meaningful for various applications.

1. Introduction

Laser sources operating at 2.0- μm wavelength range have attracted growing interest in view of a wide variety of emerging scientific and technological applications, such as range-finding, coherent laser radar, atmospheric sensing [1,2]. Moreover, this wavelength range has important applications in medicine because of large absorption coefficient of radiation at these wavelengths in water.

It is well-known that trivalent Tm³⁺ and Ho³⁺ laser materials are especially advantageous because they have wide gain spectra around 2.0 μm . In general, Ho³⁺ lasers operate at wavelengths close to 2.1 μm , e. g. Ho:YAG at 2.09 μm [3] and Ho:YAP at 2.11 μm [4], while Tm³⁺ lasers operate at wavelengths close to or less than 2 μm [5–11]. Some Tm³⁺ lasers could also be wavelengths tuned to close to 2.1 μm via some specific methods. For instance, Tm:YAG lasers can be wavelength tuned to as far as 2.16 μm and the lasing wavelength of Tm:YSGG can be tuned to 2.14 μm [12]. Feng et al. [13] reported wavelength tuned Tm:Lu₂SiO₅ lasers with wavelength extended to 2.07 μm . Tm:KY(WO₄)₂ lasers are also possible to be operated at this long wavelength [14]. Recently, Beyatli et al. [15] has reported three wavelength tunable lasers based on Tm:YLF crystal (with wavelength tuned to about 2.04 μm), Tm:LuAG

crystal (to about 2.11 μm) and Tm:YAG crystal (to about 2.09 μm). Researches on wavelength extensions are practically meaningful and necessary, which extend the applications of them as laser sources.

Tm:LiYF₄ (YLF) is a well-know Tm³⁺-doped fluorides. It has several main emission peaks between 1.8 and 1.9 μm and the emission intensity of it drops to very weak at close to 2.1 μm [16]. As a result, this crystal has often been operated at wavelengths shorter than 1.9 μm [17,18]. Until recently, as mentioned above, Tm:YLF crystal laser has been found possible to lase at 2.04 μm with the aid of birefringent filter [15]. However, any inserter into the laser cavity for wavelength tuning will lead to extra loss, unavoidably.

In this work, using specifically coated end-face mirrors that suppress the high-gain 1.9 μm emission band and support laser emission at wavelengths longer than 2.05 μm , we have demonstrated a wavelength tunable Tm:YLF laser from about 2.01 to about 2.1 μm . Moreover, since the coating contains a high reflection at 2.3 μm , we have consequently operated a simultaneous dual-wavelength laser at 2.05 and 2.3 μm . Passively Q-switched laser operation has also been realized at this long wavelength of 2.05 μm using a Cr:ZnSe saturable absorber.

* Corresponding author.

** Corresponding author.

E-mail addresses: xubin@xmu.edu.cn (B. Xu), yhang@siom.ac.cn (Y. Hang).

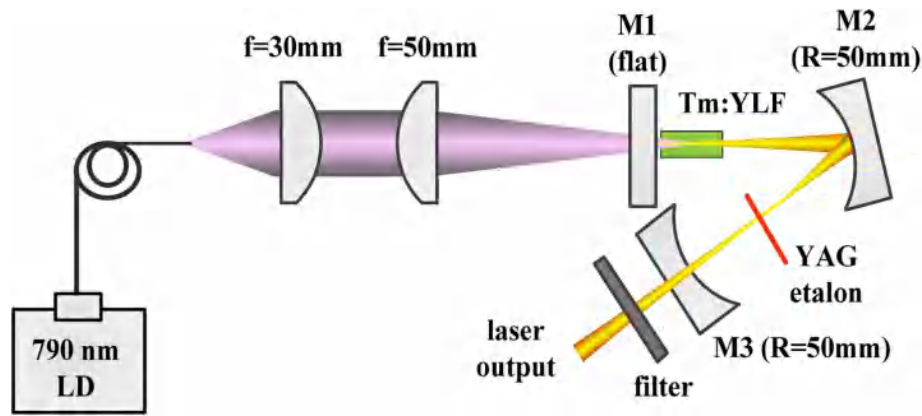


Fig. 1. Schematic of diode-pumped Tm:YLF lasers in CW and passively Q-switched regimes.

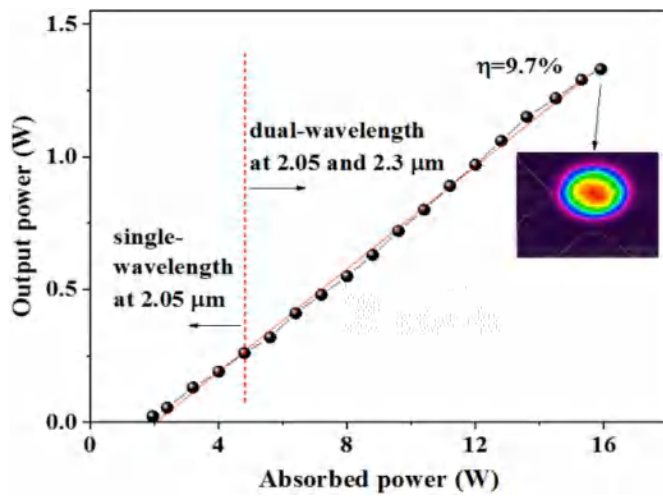


Fig. 2. The output power versus absorbed power of CW Tm:YLF laser; inset: laser beam spot at maximum output power.

2. Experimental details

Schematic of the experimental setup is shown in Fig. 1. A fiber-coupled diode laser served as pump source emitting at 790 nm with core diameter of 105 μm and numerical aperture of 0.22. The pump beam was collimated by a 30-mm (focal length) doublet lens and then focused by a 50-mm doublet lens into the laser crystal. A three-mirror V-shaped laser resonator was arranged with a flat input mirror M1, a 50-mm (curvature radius) concave mirror M2 and another 50-mm concave mirror M3. The M1 has a high transmission of about 90% at pumping wavelength and a high-reflection of about 99.8% at considered laser wavelengths. The M2 has the same coating as that of M1. The M3, acting as output coupler, has a flat transmission from 2.05 to 2.3 μm with specific values of about 0.98% at 2.05 μm and 1.83% at 2.3 μm . Beyond this range, i.e. shorter than 2.05 μm and longer than 2.3 μm , transmission of the M3 sharply increases, e.g. to about 78% at 1.9 μm and 12% at 2.01 μm .

The laser gain medium is an *a*-cut Tm:YLF crystal with dopant concentration of 4 at.% and dimensions of $3 \times 3 \times 11 \text{ mm}^3$ (11 mm along the cavity axis). It absorbs about 82.4% of the pump power, which led to an effective absorption coefficient of about 1.58 cm^{-1} . To protect the

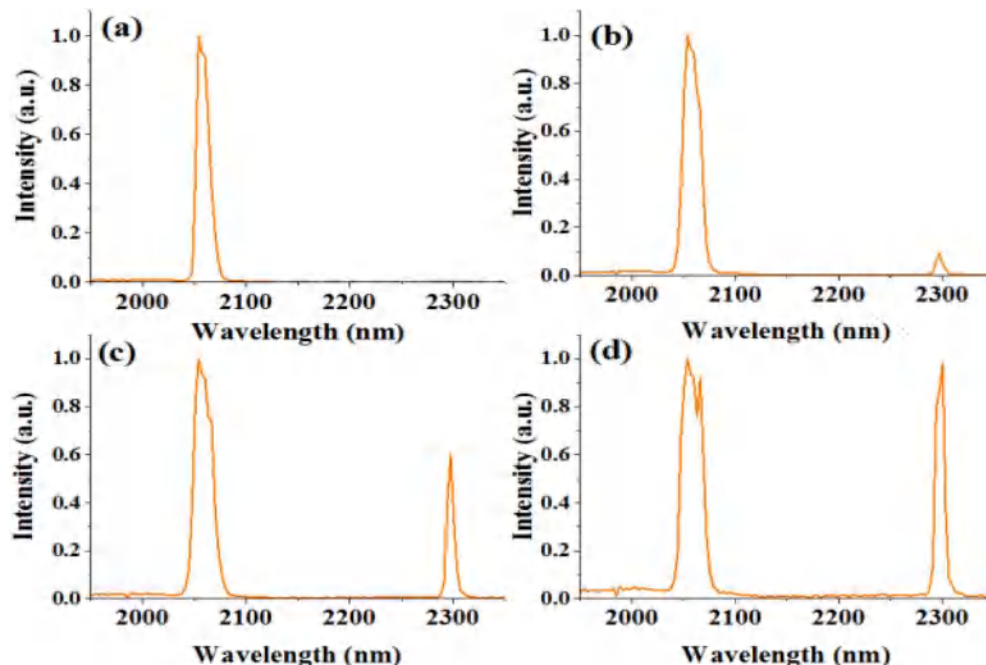


Fig. 3. Typical laser spectra at output powers of (a) below 0.26 W, (b) 0.32 W, (c) 0.48 W and (d) 1.33 W.

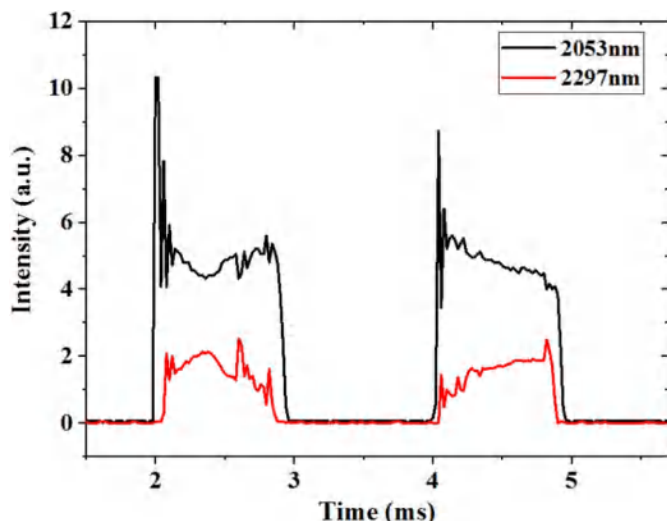


Fig. 4. Temporal behaviors of the separated 2053 and 2297 nm lasers.

laser crystal from thermal fracture, it was wrapped with indium foil and then mounted inside a water-cooled copper block with temperature set at 14 °C. In this experiment, an undoped YAG thin plate with thickness of 0.13 mm was used as Fabry-Pérot etalon for wavelength tuning, which was inserted between M2 and M3. For the operation of passive Q-switching, the YAG etalon was replaced by an anti-reflection coated Cr:ZnSe saturable absorber with initial transmission of about 88%.

3. Results and discussion

Without the insertions of the YAG etalon and Cr:ZnSe saturable absorber, a continuous-wave laser operation has been achieved after good alignment of the laser resonator. The dependence of output power on absorbed power is shown in Fig. 2. The laser threshold is about 1.95 W and with the increasing of the absorbed power to about 15.9 W the maximum output power almost linearly promoted to about 1.33 W. Linear fit of the output power data leads to a slope efficiency (η_s) of about 9.7%. We estimate the intracavity round-trip loss L using the following expression:

$$\eta_s = \frac{\lambda_p}{\lambda_o} \eta_p \frac{T}{T + L}$$

where λ_p is the pumping wavelength, λ_o is the laser wavelength, T is the transmission of the output coupler and η_p is the excitation quantum efficiency, i.e. the fraction of excited ions per absorbed pump photons, which can be assumed to be equal to 1. Thus, using the above data, we can calculate the intracavity round-trip loss to be about 3.0%, which mainly arises from the non-anti-reflection coating, imperfect quality and reabsorption loss of the laser crystal.

By monitoring the laser wavelength, we found that below an output power of about 0.26 W only single-wavelength at about 2053 nm can be achieved. However, further increasing the pump power, a new wavelength at about 2297 nm can also lase. As a consequence, in this experiment a simultaneous dual-wavelength lasing behavior at 2053 and 2297 nm occurred. We have shown the wavelength evolution at different output powers, as shown in Fig. 3. As reported above that the maximum output power is about 1.33 W and the corresponding lasing wavelength is shown in Fig. 3(d), the output powers are determined to be about 1.14 W and 0.19 W for the 2053 nm and 2297 nm lasers, respectively, using two partial transmission filters. In this experiment, we further verified the temporal synchronization of the two wavelengths by monitoring the two separated lasers with two photodiodes and an oscilloscope. Note that at this time the pump beam was modulated by a mechanical chopper. The oscillogram is shown in Fig. 4.

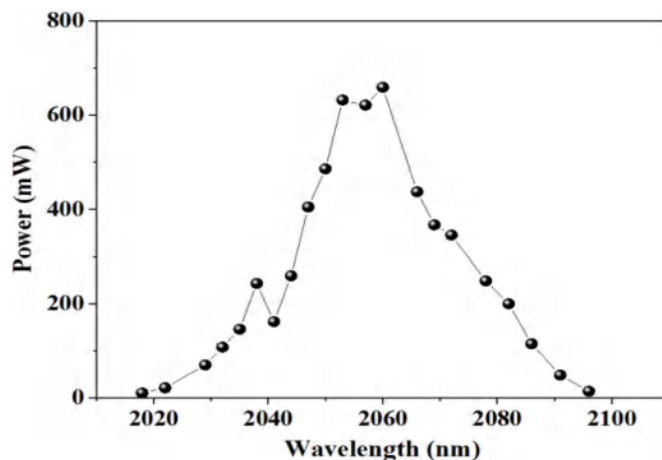


Fig. 5. The laser wavelength tunability from 2018 to 2096 nm.

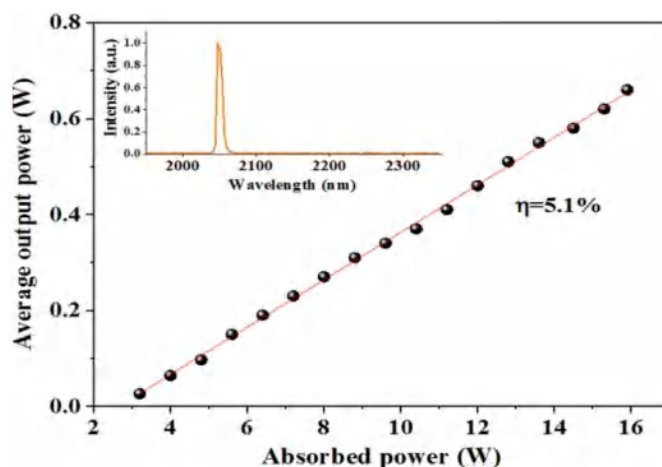


Fig. 6. The average output power versus absorbed power of the passively Q-switched Tm:YLF laser; inset: the corresponding laser spectrum at 2047 nm.

Ref. [18] reported a continuous-wave Tm:YLF laser at 1902 nm with a maximum output power 4.5 W and slope efficiency of 17%. According to Ref. [16], emission cross section of the 2.05 μm line is far less than that of commonly studied 1.9 μm line. However, in this experiment, we have still achieved considerable laser output power and slope efficiency, which should be attributed to a weak negative influence of reabsorption effect. As we know, Tm³⁺ lasers corresponding to $^3F_4 \rightarrow ^3H_6$ transition belong to quasi-three level system. Laser performances of quasi-three level lasers are in general limited by reabsorption losses of the laser materials. The relatively small round-trip loss according to the above estimation could indicate that the reabsorption loss is also very small. Furthermore, according to the absorption spectrum of Tm:YLF crystal reported in Ref. [16], in fact, the reabsorption effect of Tm:YLF crystal only exists below 2.0 μm .

Wavelength tuning was fulfilled with the YAG etalon. Under the present case, by slightly tilting the YAG etalon, we found the wavelength can be tuned from 2018 nm to 2096 nm, i.e. a wavelength range of 78 nm, as shown in Fig. 5. Achieving shorter wavelength is limited by the high transmission loss of the output coupler, while very low gain should answer for the no lasing at longer wavelength. Note that we operated the wavelength tuning at an absorbed power of about 14 W during the wavelength tuning. Above this absorbed power to a maximum absorbed power of 15.9 W, weak 2.3- μm laser emission can also be observed sometimes.

Replacing the YAG etalon with the Cr:ZnSe saturable absorber and

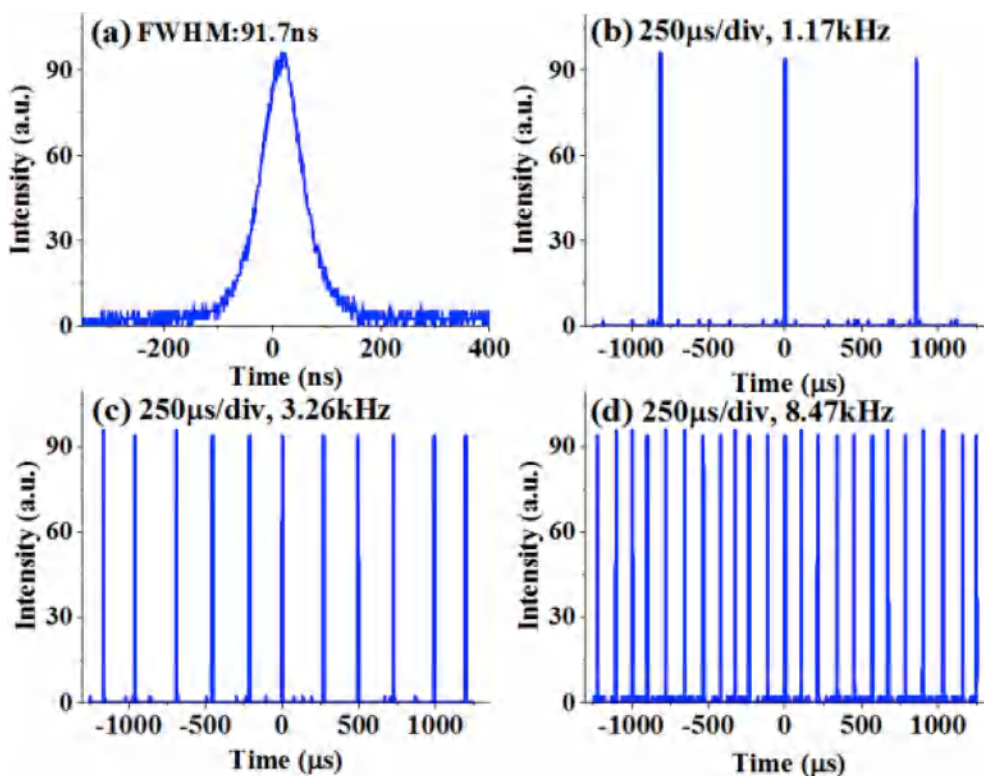


Fig. 7. (a) The achieved shortest pulse width and (b–d) pulse trains at repetition rates of 1.17 kHz, 3.26 kHz and 8.47 kHz.

increasing the absorbed power to about 3.2 W, a stable passively Q-switched laser operation was obtained with a maximum average output power of 0.66 W, as shown in Fig. 6. Note that the 3.2 W absorbed power only allowed single wavelength lasing at 2053 nm for continuous-wave case. The slope efficiency is about 5.1%. The laser wavelength was found to be about 2047 nm (see the inset in Fig. 6). Comparing with continuous-wave case, 2.3 μm laser emission has not appeared, which can be explained as follows. According to the absorption spectrum of Cr:ZnSe crystal [19], the absorption coefficient at 2.05 μm is still considerable to be about close to 2 cm^{-1} , while it drops to be negligible at 2.3 μm. That is to say, the Cr:ZnSe crystal is much more easier to be saturated at 2.05 μm than at 2.3 μm. Moreover, in continuous-wave mode, 2.05 μm laser emission dominated inside the laser cavity despite simultaneous dual-wavelength laser operation. As a result, the 2.05 μm emission line oscillated in passively Q-switched mode while the 2.3-μm transition line has been suppressed.

For a passively Q-switched laser operation, theoretical pulse width τ can be estimated using the following equation [20].

$$\tau = 3.52 \frac{t_r}{q_0}$$

where t_r is the cavity round-trip time and q_0 is the modulation depth of the used Cr:ZnSe saturable absorber. Using this formula, we can simply calculate the modulate depth to be about 2.4%. Hence, on the other hand, by increasing the modulation depth, we expected pulse width of the Q-switched laser at 2047 nm can be further narrowed.

The achieved laser pulses in different temporal scale are reported in Fig. 7. In this experiment, the shortest pulse width is about 91.7 ns (see Fig. 7(a)). Fig. 7(b–d) shows the typical pulse trains at threshold, 0.23 W and maximum of average output powers with repetition rates of 1.17 kHz, 3.26 kHz and 8.47 kHz, respectively. Stability of the passively Q-switched laser was estimated to be less than about 9.2% by measuring the pulse-to-pulse amplitude fluctuation. Moreover, during the laser experiment, we found that with the increasing of the absorbed power the pulse repetition rate increased quite linearly. Finally, the maximum

pulse energy was estimated to be about 77.9 μJ and the pulse peak power to be about 0.85 kW.

4. Conclusion

We have demonstrated a simultaneous dual-wavelength laser at 2.05 and 2.3 μm with a maximum output power of 1.33 W and slope efficiency of about 9.7% in continuous-wave regime. The 2.05 μm lasing wavelength can be shifted from 2.01 μm to 2.1 μm by using an un-doped YAG etalon for wavelength tuning. Using a Cr:ZnSe saturable absorber, a passively Q-switched Tm:YLF laser at 2.05 μm was also obtained with a maximum average output power of 0.66 W. The shortest pulse width is 91.7 ns at pulse repetition rate of 8.47 kHz, which led to pulse energy of 77.9 μJ and a pulse peak power of 0.85 kW.

Suppression of the 2.01–2.1 μm lasing by high-transmission coating at this emission band will lead to a single-wavelength Tm:YLF laser at 2.3 μm, which is especially of interest in gas detection systems. The 2.3 μm laser radiation can also be obtained in a broadly tunable Cr:ZnSe laser. However, 2.3-μm Tm:YLF laser is still advantageous because its pump source can be provided by a compact, high-power and cost-effective 790-nm diode laser. As we know, Cr:ZnSe laser should be pumped by a costly and complex Tm³⁺ laser at 1.9 μm.

Conflicts of interest

The authors declare no conflicts of interest.

Acknowledgments

This work is supported in part by National Natural Science Foundation of China (61575164, 51872307) and Natural Science Foundation of Fujian Province of China (2018J01108).

References

- [1] F. Gibert, D. Edouart, C. Cenac, F. Le Mounier, 2- μm high-power multiple-frequency single-mode Q-switched Ho:YLF laser for DIAL application, *Appl. Phys. B* 116 (2014) 967–976.
- [2] S.R. Bowman, C. Baker, G. Villalobos, B. Shaw, B. Sadowski, M. Hunt, I. Aggarwal, J. Sanghera, Holmium doped laser materials for eye-safe solid state laser application, *Proc. SPIE* 9081 (2014) 908105.
- [3] S. So, J.I. Mackenzie, D.P. Shepherd, W.A. Clarkson, J.G. Betterton, E.K. Gorton, J. A.C. Terry, Intra-cavity side-pumped Ho:YAG laser, *Opt. Express* 14 (22) (2006) 10481–10487.
- [4] B.Q. Yao, X.M. Duan, L.L. Zheng, Y.L. Ju, Y. Wang, G.J. Zhao, Q. Dong, Continuous-wave and Q-switched operation of a resonantly pumped Ho:YAlO₃ laser, *Opt. Express* 16 (19) (2008) 14668–14674.
- [5] J.F. Pinto, L. Esterowitz, G.H. Rosenblatt, Continuous-wave mode-locked 2- μm Tm:YAG laser, *Opt. Lett.* 17 (1992) 731–733.
- [6] J.L. Lan, B. Xu, Z.Y. Zhou, H.Y. Xu, Z.P. Cai, X.D. Xu, J. Xu, R. Moncorgé, High-Power CW and Q-switched Tm:CaYAlO₄ lasers at 1.94 μm for shallow water absorption, *IEEE Phot. Tech. Lett.* 29 (2017) 2127–2130.
- [7] J. Liu, Y.G. Wang, Z. Qu, X. Fan, 2 μm passive Q-switched mode-locked Tm³⁺:YAP laser with single-walled carbon nanotube absorber, *Opt. Laser. Technol.* 44 (2012) 960–962.
- [8] Y. Wang, J.L. Lan, Z. Zhou, X. Guan, B. Xu, H.Y. Xu, Z.P. Cai, Y. Wang, Chaoyang Tu, Continuous-wave laser operation of diode-pumped Tm-doped Gd₃Ga₅O₁₂ crystal, *Opt. Mater.* 66 (2017) 185–188.
- [9] Y.F. Li, B.Q. Yao, Y.Z. Wang, Diode-pumped CW Tm:GdVO₄ laser at 1.9 μm , *Chin. Opt. Lett.* 4 (2006) 175–176.
- [10] P. Camy, J.L. Doualan, S. Renard, A. Braud, V. Menard, R. Moncorgé, Tm³⁺:CaF₂ for 1.9 μm laser operation, *Opt. Commun.* 236 (2004) 395–402.
- [11] C. Zhang, J. Liu, X.W. Fan, Q.Q. Peng, X. Guo, D.P. Jiang, X. Qian, L.B. Su, Compact passive Q-switching of a diode-pumped Tm,Y:CaF₂ laser near 2 μm , *Opt. Laser. Technol.* 103 (2018) 89–92.
- [12] R.C. Stoneman, L. Esterowitz, Efficient, broadly tunable, laser-pumped Tm:YAG and Tm:YSGG cw lasers, *Opt. Lett.* 15 (9) (1990) 486–488.
- [13] T. Feng, K. Yang, S. Zhao, J. Zhao, W. Qiao, T. Li, L. Zheng, J. Xu, Broadly wavelength tunable acousto-optically Q-switched Tm:Lu₂SiO₅ laser, *Appl. Opt.* 53 (27) (2014) 6119–6122.
- [14] A.A. Lagatsky, S. Calvez, J.A. Gupta, V.E. Kisel, N.V. Kuleshov, C.T.A. Brown, M. D. Dawson, W. Sibbett, Broadly tunable femtosecond mode-locking in a Tm:KYW laser near 2 μm , *Opt. Express* 19 (10) (2011) 9995–10000.
- [15] E. Beyatli, U. Demirbas, Widely tunable dual-wavelength operation of Tm:YLF, Tm:LuAG, and Tm:YAG lasers using off-surface optic axis birefringent filters, *Appl. Opt.* 57 (23) (2018) 6679–6686.
- [16] B.M. Walsh, N.P. Barnes, B.D. Bartolo, Branching ratios, cross sections, and radiative lifetimes of rare earth ions in solids: application to Tm³⁺ and Ho³⁺ ions in LiYF₄, *J. Appl. Phys.* 83 (5) (1998) 2772–2787.
- [17] W. Bolanos, F. Starecki, A. Benayad, G. Brasse, V. Ménard, J.L. Doualan, A. Braud, R. Moncorgé, P. Camy, Tm:LiYF₄ planar waveguide laser at 1.9 μm , *Opt. Lett.* 37 (19) (2012) 4032–4034.
- [18] Y. Dai, Y. Li, X. Zou, B. Jiang, Y. Hang, Y. Leng, Compact passively Q-switched Tm:YLF laser with a polycrystalline Cr:ZnS saturable absorber, *Opt. Laser. Technol.* 57 (2014) 202–205.
- [19] A.V. Podlipensky, V.G. Shcherbitsky, N.V. Kuleshov, V.P. Mikhailov, V. I. Levchenko, V.N. Yakimovich, Cr²⁺:ZnSe and Co²⁺:ZnSe saturable-absorber Q switches for 1.54-mm Er:glass lasers, *Opt. Lett.* 24 (14) (1999) 960–962.
- [20] G.J. Spuhler, R. Paschotta, R. Fluck, B. Braun, M. Moser, G. Zhang, E. Gini, U. Keller, Experimentally confirmed design guidelines for passively Q-switched microchip lasers using semiconductor saturable absorbers, *J. Opt. Soc. Am. B* 16 (3) (1999) 376–388.